Journal of Computer-Aided Molecular Design, 6 (1992) 303–314
ESCOM

J-CAMD 163

Quantum chemical study on the interaction of some bisphosphonates and Ca^{2+}: The role of molecular electrostatic potentials in the prediction of binding geometry

J.-P. Björkroth[a,*], M. Peräkylä[a], T.A. Pakkanen[a] and E. Pohjala[b]

[a]*University of Joensuu, Department of Chemistry, P.O Box 111, 80101, Joensuu, Finland*
[b]*Huhtamäki Oy Leiras, P.O. Box 415, 20101 Turku, Finland*

Received 7 November 1991
Accepted 13 April 1992

Key words: Bisphosphonates, Molecular electrostatic potentials; Calcium binding

SUMMARY

Molecular electrostatic potentials have been used to model the calcium binding properties of some bisphosphonate drugs, which are used to treat various bone diseases. The mechanism of action involves the binding of bisphosphonates to the bone surface, where calcium plays an important role. Electrostatic potential maps derived from ab initio partial charges have been compared with both the crystal structure and the fully optimized ab initio structure of (dichloro)methylenebisphosphonate–calcium ion complex. Molecular electrostatic potentials can correctly predict the calcium binding geometry of bisphosphonate-type compounds and this type of information can be used in the practical drug design work.

INTRODUCTION

1. The electrostatic potentials

The prediction of binding geometries and energies in receptor–ligand interactions are often important in drug design. If the system is small enough, very precise quantum chemical methods can be used to obtain molecular geometries and to study the energetics of binding. In practical drug design, however, this is rarely the case; the size of a full receptor–ligand system may be very large and this limits the number of theoretical methods that can be used. Normally the receptor is a large macromolecule, like a protein, and due to its size the whole structure cannot be modelled with quantum chemical methods and the system under research has to be reduced to the smallest reasonable model which can still describe the interaction accurately enough [1]. The calculation of an ab initio wave function ('the single point calculation') is usually possible in reasonable time

*To whom correspondence should be addressed at: Technical Research Centre of Finland, Chemical Laboratory, P.O. Box 204, SF-02151, Espoo, Finland.

with minisupercomputers or workstations, but if the full geometry optimization is to be performed for systems larger than 15 to 20 heavy atoms, the calculation time may become too long for practical purposes even with the fastest supercomputers. This is especially the case if an interaction between two or more separate molecules is to be studied and the geometry of this kind of system is to be optimized with ab initio methods.

In practice it is not always necessary to optimize the whole electronic structure by quantum chemical methods if interactions between two or more molecules are to be studied. Instead, the molecular electrostatic potentials (MEP) [2] can be used. The nuclear and electronic charge distribution of the molecule creates an electrostatic potential, which will interact with the electron density of another molecule or, for example, a point charge. Between two charged particles (atoms, molecules) there is always an electrostatic interaction [3], and in the drug–receptor recognition and docking processes, the regions of opposite molecular electrostatic potentials in drug and receptor should match [4]. Also, with a set of ligands having affinity to the same receptor, the electrostatically similar groups should be orientated in the binding process in a similar manner [5]. These facts make the electrostatic potentials valuable tools in the theoretical research of drug–receptor interactions with computational techniques, and electrostatic potentials are used frequently in the field of drug design [6].

A comprehensive list of examples of the use of electrostatic potentials in drug design can be found in ref. [2].

It has to be mentioned, that the results of these electrostatic potential based interaction studies are always approximations when compared with full interaction calculations using methods of theoretical chemistry; normally the effect of these electrostatic fields on each other and the changes in geometries in binding processes are not taken into account in the first stage of the study, when molecular electrostatic potential maps are calculated for separate molecules prior to the interaction process itself. The next stage in a molecular electrostatic potential study may be the calculation of the interaction potentials to evaluate the binding energy when the two molecules are in equilibrium geometry [7]. When the energetics of the interaction are to be studied, one should be careful when the electrostatic potentials are the only tools to evaluate the interaction, since the results are only suggestive when compared with the results of energy calculations from a quantum chemical or force field method. Electrostatic potentials are still very useful tools in understanding the particular interaction, when these more accurate (and sometimes much slower!) methods cannot be used.

The electrostatic potential at any point r in space can be expressed by Eq. 1:

$$V(\mathrm{r}) = \sum_{\mathrm{A}} \frac{Z_{\mathrm{A}}}{|R_{\mathrm{A}} - r|} - \int \frac{\rho(r')\,\mathrm{d}r'}{|r' - r|} \tag{1}$$

where Z_{A} is the charge at nucleus A located at R, and $\rho(r')$ is the electronic density function at position r'. The first term represents the nuclear contribution and the second term is the electronic contribution. The electronic density function used in the calculation of the potential may be obtained from quantum chemical calculations.

In those cases, where the wave function of the molecule is not available, the molecular electrostatic potential can be calculated from point charges of the atoms of a molecule. If the partial charge method is to be used, it is very important to note from where the partial charges of the

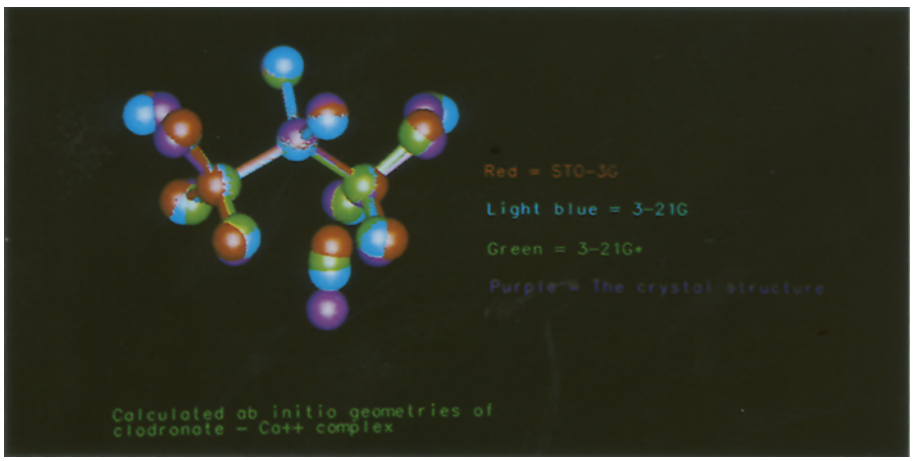

Fig. 1. The comparison of STO-3G, 3-21G and 3-21G(*) optimized structures of the clodronate–Ca^{2+} complex and the crystal geometry.

atoms are obtained. There is a variety of different empirical methods for point charge calculations [8–12], but the results are not as accurate as the results from the wave function based methods [13]. It has to be mentioned that the method to obtain reasonable partial charges depends heavily on the structure and environment of the molecules in question.

Often in practical work with commercial molecular modeling software packages and quantum chemical programs, the point charges are obtained by Mulliken population analysis [14] of the wave function, and molecular electrostatic potentials are derived from these point charges. Here some attention should be paid to the atomic charges and electrostatic potentials derived from these partial charges [15]. The population analysis is based on the coefficients of the atomic orbitals in the individual molecular orbitals, and diffuse orbitals may perform functions other than those for which they are intended. If they are used to improve the description of an atom other than the one on which they are centered, the population of the orbital involved is assigned to the atom on which it is centered and not to the one that is actually using the basis function [16], and this may affect the partial charges of the individual atoms. The charges are also often very basis-set-dependent. This suggested to us to compare the Mulliken charge-based electrostatic potentials with those derived from a wave function. According to our results, the molecular electrostatic potentials derived from ab initio Mulliken charges are accurate enough for practical, qualitative studies in order to predict the interaction geometry reasonably well, and also to give some guidance as to the energetics of binding in the interaction of Ca^{2+} with various phosphonates.

2. *Bisphosphonates*

In this paper some bisphosphonates and their calcium binding properties have been studied. Bisphosphonates are compounds characterized with a P-C-P system:

Bisphosphonic acid, dianion

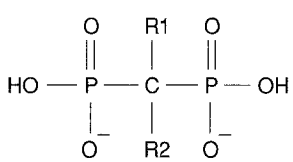

(Dichloromethylene)bisphosphonate, (clodronate) R1= R2= Cl

These compounds have a high affinity to bone, and they have been used in the treatment of various bone and tooth diseases. The detailed mechanism of action of these drugs is still unknown, but it is known that bisphosphonates bind to the surface of bone, and presumably some cellular mechanisms are also involved [17]. Bisphosphonates have a high affinity for calcium phosphate [18] and they inhibit both the formation [19] and dissolution [20] of this mineral. These compounds are also powerful inhibitors of bone resorption, both in vivo and in vitro [17].

In this work we have calculated the interaction geometries of (dichloromethylene)bisphosphonate (clodronate) and a calcium ion by ab initio methods with different basis sets, and compared the results with the molecular electrostatic potentials of clodronate and of various molecules derived from clinically used bisphosphonate compounds. The model mechanism of action in this study is the binding of the Ca^{2+} ion to bisphosphonate, which is the major interaction in the binding of these drugs to the bone surface.

METHODS

The calculations performed in our laboratory were done with Gaussian-88 and Gaussian-90 [21] ab initio molecular orbital programs running in VAX-6140 and in Cray-XMP with the default gradient procedure. The crystal structure of the clodronate–Ca^{2+} complex (clodronic acid calcium salt, pentahydrate) was taken from the work of Nardelli and Pellizzi [22]. The whole complex was fully optimized with basis sets STO-3G, 3-21G and 3-21G(*) at the Hartree–Fock level. The split valence basis sets 3-21G and 3-21G(*) for calcium were taken from the work of Dobbs and Hehre [23]. In the 3-21G(*) calculation, six sets of d-orbitals were used. The smaller basis sets

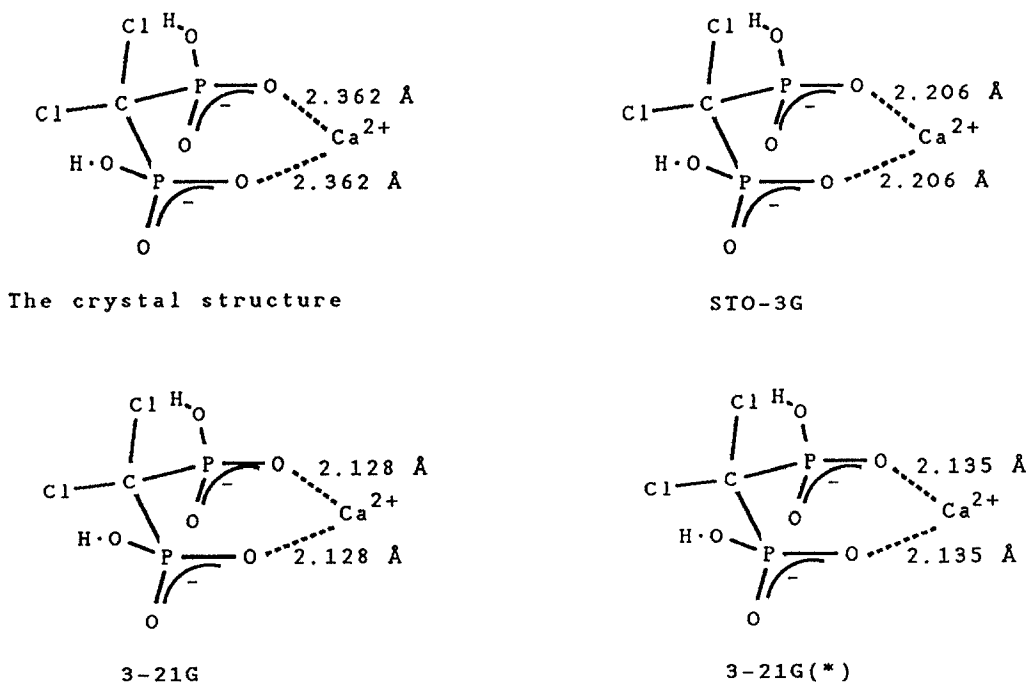

Fig. 2. The binding distance of Ca^{2+} from phosphonate non-OH oxygens in calculated models and in the crystal structure.

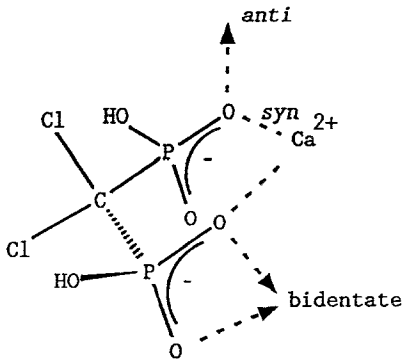

Fig. 3. The binding conformation and stereochemical designation in the phosphonate–Ca^{2+} interaction. Note the unfavorable *anti* interaction and unfavorable bidentate binding mode in both separate phosphonate groups, which both interact as unidentate ligands. The binding is bidentate between the whole bisphosphonate molecule and Ca^{2+}

were included as standard in the Gaussian programs. The full clodronate molecular electrostatic potential maps were derived after full geometry optimization of the clodronate dianion for each of the three basis sets. The partial charges obtained by the Mulliken population analysis were used in deriving the molecular electrostatic potential maps. Also, the ab initio geometries of the full complex were compared with the crystal structure. All calculations are for 0 K structures; the possible influences of temperature and entropy are not included.

The 'half-molecule' approach was used with the set of different phosphonate and phosphinate compounds derived from clodronate and other similar type of drugs. The studied structures were derived from the parent bisphosphonate compound by replacing one phosphonate group with hydrogen. These molecules were not optimized, but the crystal geometry of clodronate was used and the partial charges were computed with either 3-21G(*) or 6-31G* basis sets. The atomic point charges were used to derive the electrostatic potential maps.

All the molecular building work and displaying of the results were done with a Sybyl 5.32 or 5.41 molecular modeling program [24] running on Evans and Sutherland PS390, and Microvax-II or Evans and Sutherland ESV20 system.

RESULTS AND DISCUSSION

The comparison of STO-3G, 3-21G and 3-21G(*) optimized structures of the clodronate–Ca^{2+} complex, and the crystal geometry is shown in Fig. 1. All three basis sets seem to describe the bond lengths, angles and torsions in the clodronate anion quite similarly. No significant variation in these structural parameters can be found. The difference in $Ca^{2+}...O^{-}$ binding distance between calculated model structures and the crystal structure varies from 0.16 Å to 0.23 Å (Fig. 2); in all the models it is shorter than in the crystal structure. This is due to the influence of the uncomplete coordination sphere of Ca^{2+} in the calculated models [25]; the coordination number of Ca^{2+} is only 2 in these models and 7 in the crystal structure. The binding of the calcium ion in all the calculated structures occurs in the plane of $^{-}$O-P-C-P-O^{-} in the nearly eclipsed conformation (Fig. 3). This is similar to the situation in the crystal structure. This suggests that symmetrical bidentate monophosphonate–metal ion interaction is unfavourable relative to an unidentate, *syn* geometry. The interaction between one separate phosphonate group and Ca^{2+} however, is unidentate, and

the whole bisphosphonate could act as a bidentate ligand (double unidentate) in Ca^{2+} binding. The observed unidentate binding of Ca^{2+} to the phosphonate group is in complete accordance with the study of Alexander et al. on the stereochemistry of phosphate-Lewis acid interactions [26]. Also, Deerfield et al. have found a similar unidentate binding geometry between Ca^{2+} and malonate in their recent quantum mechanical study [27]. The basic arrangements in malonate and bisphosphonate are very similar and support our results about the binding geometry, although the Ca^{2+}...O distances in carboxylates are shorter than those in phosphonates.

a

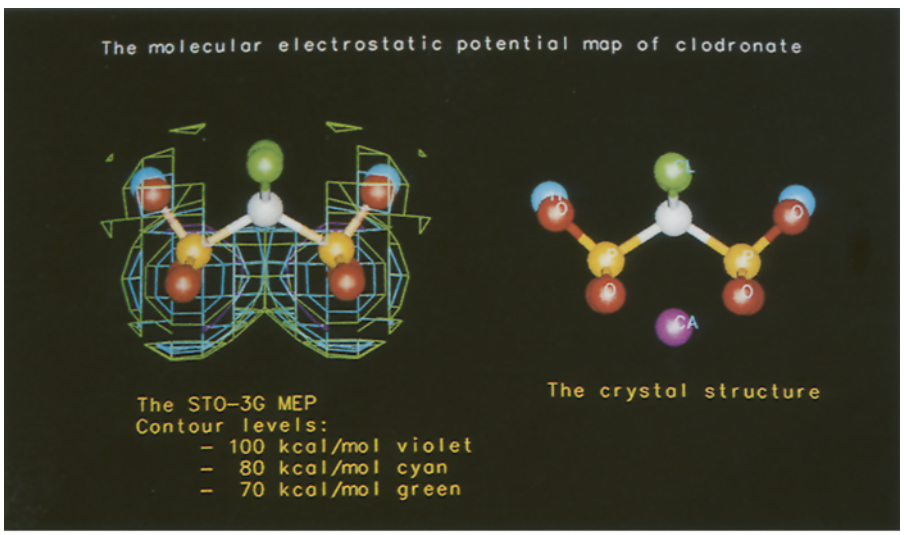

b

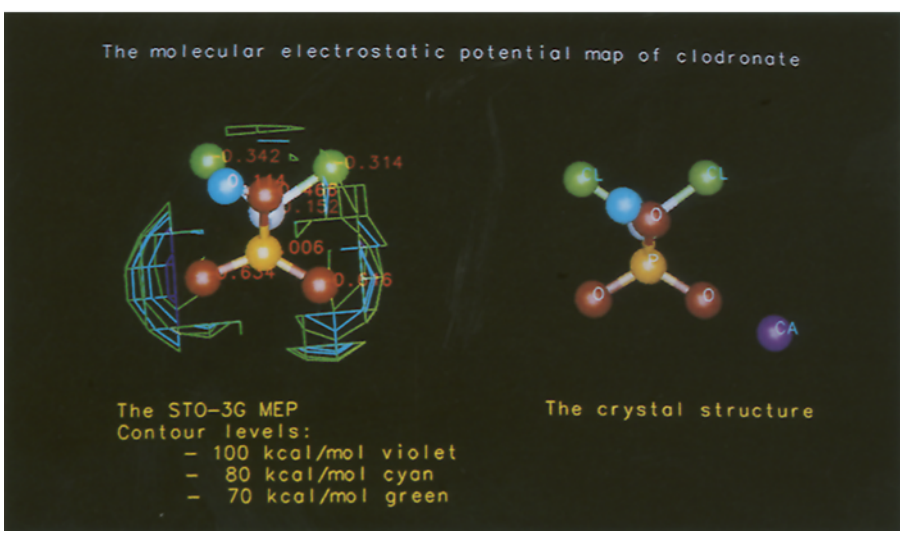

Fig. 4. (a and b) The orthogonal view of the STO-3G-based MEP map of clodronate. The contour levels are −100 kcal/mol (violet), −80 kcal/mol (cyan) and −70 kcal/mol (green).

The interaction energies between Ca^{2+} and the clodronate anion in the full complex models are: STO-3G, −591.2 kcal/mol; 3-21G, −493.3 kcal/mol; and 3-21G(*), −518.9 kcal/mol. These energies are not corrected for the BSSE, since in this study the absolute values of interaction energies are of minor importance. Maynard et al. report BSSE corrections of 15–28% to the minimal basis set for a Ca ion and ligand systems [28], but according to Shiratori and Nakagawa the BSSE for split valence basis sets are much better [25]. The non-BSSE-corrected interaction energies in their study for Ca^{2+}...$HCOO^-$ system vary from −285.5 to −335.6 kcal/mol depending on the basis

a

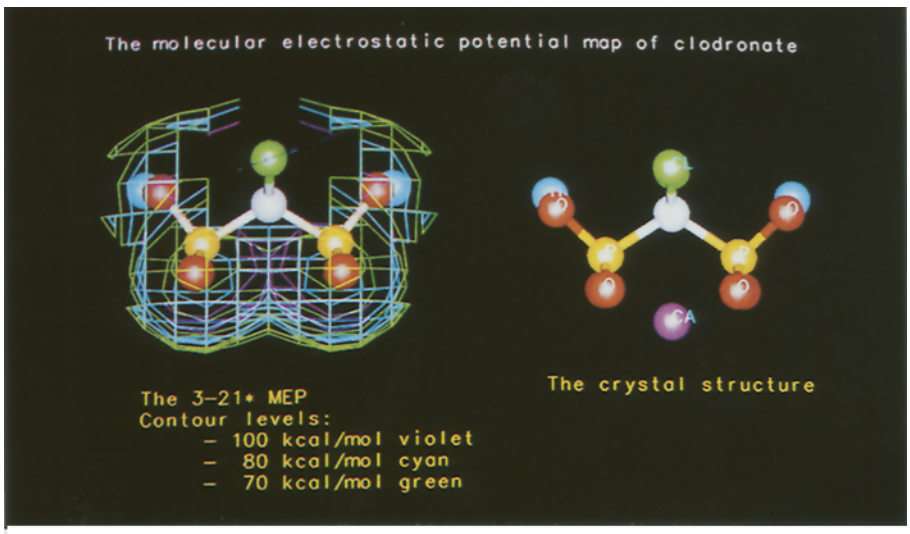

b

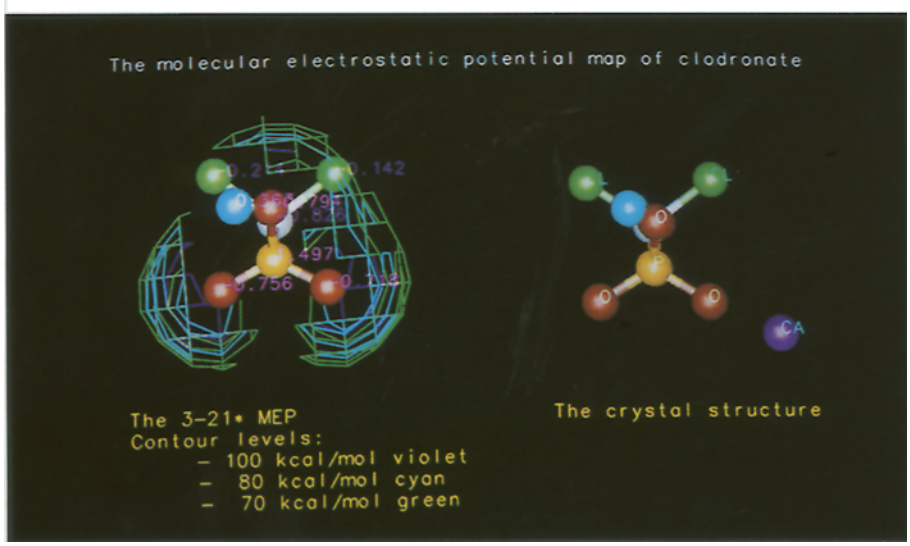

Fig. 5. (a and b) The orthogonal view of the 3-21G(*)-based MEP map of clodronate. The contour levels are −100 kcal/mol (violet), −80 kcal/mol (cyan) and −70 kcal/mol (green).

TABLE 1
COMPARISON OF THE EXACTLY CALCULATED ELECTROSTATIC POTENTIAL WITH THE POINT CHARGE APPROXIMATION (3-21G(*) BASIS SET) FOR METHYLPHOSPHONIC ACID MONOANION[a]

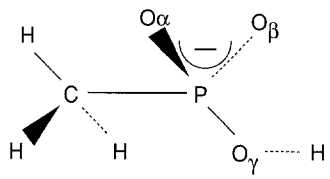

Electrostatic potential location	Point charge approximation (kcal/mol)	Exact (kcal/mol)
1.5 Å from O_α[b]	−155.6	−167.1
1.5 Å from O_β[b]	−154.2	−163.2
1.5 Å from O_γ[b]	−119.2	−109.1
1.5 Å from P[c]	−103.7	− 91.4
2.0 Å from P[d]	−137.3	−156.8
2.0 Å from P[e]	−149.9	−153.9
2.0 Å from P[f]	−106.6	− 94.0

[a] 3-21G(*) optimized geometry, torsion H–O_γ–P–C is 132.5°.
[b] Along P–O line.
[c] Along C–P line.
[d] On $O_\alpha PO_\beta$ bisector.
[e] On $O_\alpha PO_\gamma$ bisector.
[f] On $O_\beta PO_\gamma$ bisector.

set. From these results it can be seen that the interaction between bisphosphonates and Ca^{2+} is almost twice as strong as the interaction between Ca^{2+} and single carboxylates.

To validate the molecular electrostatic potentials from the Mulliken point charges we compared the electrostatic potential surrounding methylphosphonic acid monoanion as calculated from the wavefunction, with that approximated from the Mulliken charges (Table 1). In the selected points around the Ca^{2+}-binding $(HO)PO_2^-$ group the agreement is relatively good, although all the trends are not reproduced exactly. The regression equation between Mulliken (ESP(q)) and exact (ESP(ψ)) electrostatic potential values given in Table 1 is:

$$\mathrm{ESP(q)} = 0.6447\,\mathrm{ESP}(\psi) - 46.19$$
$$r^2 = 0.9536, \sigma = 4.82 \qquad (2)$$

Also the locations of the two minima of electrostatic potential inside the O-P-O angle are in agreement. In the wavefunction-derived electrostatic potential the values of the minima are −203.5 and −204.0 kcal/mol and in the same points, those derived from Mulliken charges, −210.6 and −207.8 kcal/mol, respectively. On the basis of the present comparison in this study it seems reasonable to evaluate the electrostatic potential maps using the Mulliken point charge approximation.

The electrostatic potential maps, derived from STO-3G and 3-21G(*) ab initio partial atomic charges of the clodronate dianion by the molecular modeling program SYBYL, are presented in Figs. 4 and 5. The 3-21G charge-based electrostatic potential map is very similar to the 3-21G(*) map. The most negative potential areas are located near the non-hydroxyl oxygen atoms in *syn* stereochemical designations. These negative potential valleys are those areas, into which the

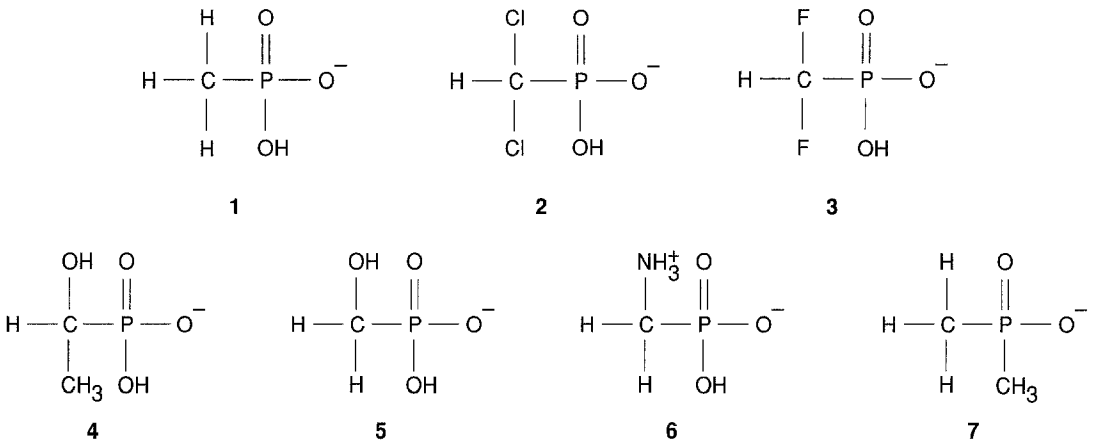

Fig. 6. The structures of analyzed 'half'-molecules. **1** Methylphosphonic acid, monoanion; **2** (Dichloromethyl)phosphonic acid, monoanion; **3** (Difluoromethyl)phosphonic acid, monoanion; **4** (1-Hydroxyethyl)phosphonic acid, monoanion; **5** (Hydroxymethyl)phosphonic acid, monoanion; **6** (Aminomethyl)phosphonic acid, zwitterion; and **7** Dimethylphosphinic acid, monoanion.

charged Ca^{2+} ion would be located. In the STO-3G electrostatic potential map, the -OH hydrogen plays a noticeable role when compared with the split-valence basis set's electrostatic potential maps, since the most negative electrostatic potential is located to the 'wrong' side of the molecule (if compared with the crystal structure), depending on the orientation of the -OH hydrogens. This effect of the -OH hydrogen seems to disappear with 3-21G and 3-21G(*) basis sets. It has to be mentioned that the orientation of the -OH hydrogens was difficult to determine with the polarization basis set, since the torsion barrier of the -OH group is rather small. Since the packing forces and hydrogen bonding are missing in the calculated models, too much attention should not be paid to the -OH torsions.

The electrostatic potential maps from the split valence basis set calculations for the clodronate dianion predict the binding area for Ca^{2+} correctly when the results are compared with the full complex calculated and the crystal structures. The 3-21G(*) basis set seems to be the best alternative for describing this interaction. This result is in accordance with our study on similar type of phosphonate group-containing compounds [29].

To see how a reduced model system can be used in describing the calcium binding properties of phosphonates, the 'half-molecule' approach was used and the results were compared with previous results. The structures studied in the 'half-molecule' approach are given in Fig. 6. As stated

TABLE 2
MINIMUM ELECTROSTATIC POTENTIAL VALUES FOR 'HALF'-MOLECULES (FIG. 6)

Molecule	Minimum electrostatic potential (kcal/mol)	Molecule	Minimum electrostatic potential (kcal/mol)
1	−121.4	**5**	−120.6
2	−112.2	**6**	− 91.1
3	−110.7	**7**	−119.3
4	−114.0		

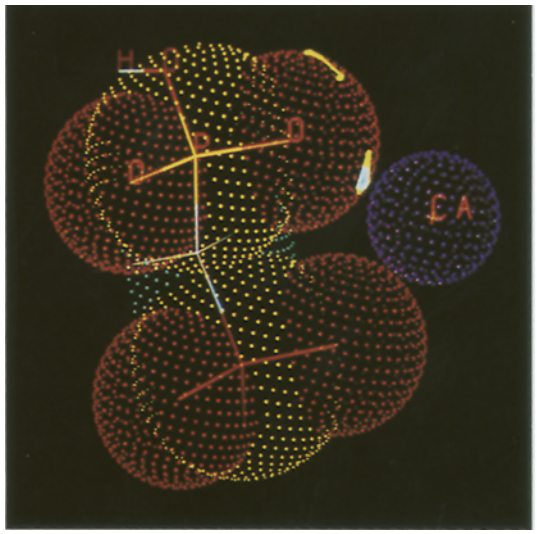

Fig. 7. The 3-21G(*) MEP map of methylphosphonic acid monoanion superimposed with the vdW surface of the crystal structure of the clodronate–Ca^{2+} complex. The contour levels are −115 kcal/mol (blue) and −110 kcal/mol (yellow).

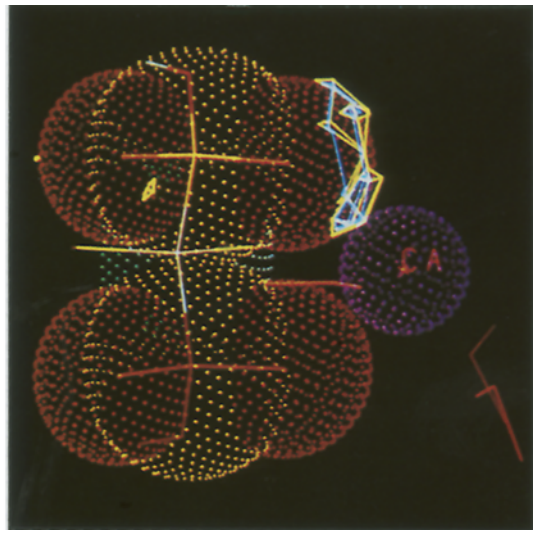

Fig 8. The 3-21G(*) MEP map of (dichloromethyl)phosphonic acid monoanion superimposed with the vdW surface of the crystal structure of the clodronate–Ca^{2+} complex. The contour levels are −101 kcal/mol (blue) and −95 kcal/mol (yellow). Three water molecules from the crystal structure are shown in red or green in Figs. 8–10.

in the methods section, the molecules were not optimized but the crystal geometry of clodronate was used and the parent substituent groups were added by using the SYBYL molecular modeling program.

For comparison, molecular electrostatic potential maps for the methylphosphonic acid monoanion computed from 3-21G(*) and 6-31G* charges were compared. Both maps were very similar, and the 3-21G(*) basis sets were chosen to be the standard basis sets in this study due to their smaller size, which shortens the calculation time.

The location of the calcium binding site was predicted very similarly in all the half-molecule models in accordance with the previous full molecule model. As an example, Figs. 7–10 depict the most negative areas of the molecular electrostatic potential maps for the four most interesting molecules in this study (molecules **1**, **2**, **4** and **7**) superimposed with the crystal structure of the clodronate–Ca^{2+} complex. It can easily be seen that the calcium binding would occur in a similar way as in the full molecule models; the same unidentate monophosphonate–metal ion *syn* binding can be seen in the nearly eclipsed conformation. This result was obtained with all seven 'half-molecules' studied here. The magnitudes of the electrostatic potentials could be used in predicting the relative strength of the interaction. In Table 2 we have listed the minimum values of the molecular electrostatic potentials for the 'half'-molecule structures. The values are all within a similar range, however, these relative values can only be compared to each other, because the solvation effects are not taken into account at this level of the theory. Solvation and desolvation of the molecules always play an essential role in interaction processes and also affect interaction energies. If the quantitative strength of the interaction between Ca^{2+} and bisphosphonates is studied, these processes should be taken into account; this was beyond the scope of this study.

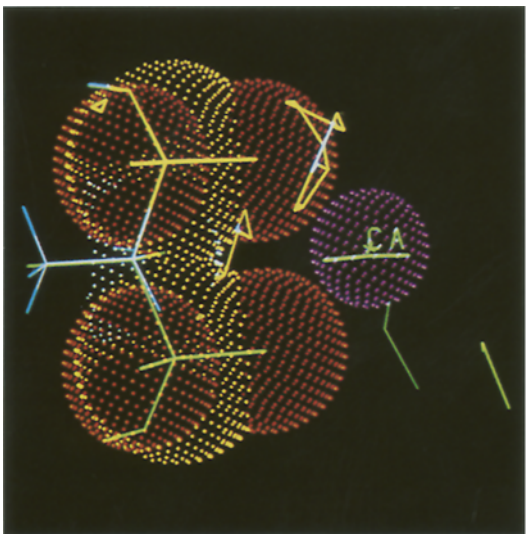

Fig. 9. The 3-21G(*) MEP map of (1-hydroxyethyl)phosphonic acid monoanion superimposed with the vdW surface of the crystal structure of the clodronate–Ca^{2+} complex. The contour levels are −110 kcal/mol (blue) and −95 kcal/mol (yellow).

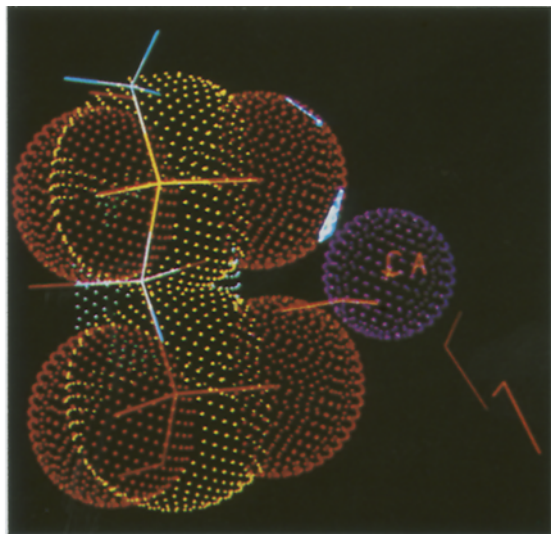

Fig. 10. The 3-21G(*) MEP map of dimethylphosphinic acid monoanion superimposed with the vdW surface of the crystal structure of the clodronate–Ca^{2+} complex. The contour levels are −110 kcal/mol (blue) and −104 kcal/mol (yellow).

CONCLUSIONS

This paper has demonstrated the possibility of using molecular electrostatic potentials to qualitatively examine ion-pair interactions. Molecular electrostatic potentials are easily obtained, valuable tools in drug design when receptor–ligand interaction is to be studied and they provide an insight into the recognition and geometry of this important chemical process. In this work electrostatic potentials obtained from ab initio partial charges correctly predicted the calcium binding site of clodronate and various other phosphonate and phosphinate compounds when compared with the crystal structure or full ab initio complex structures. According to our results, with both electrostatic potentials and ab initio calculations of the Ca^{2+}–clodronate complex, the binding of Ca^{2+} with phosphonate groups occurs in an unidentate *syn* stereochemical designation leading to a 6-membered nearly planar ring conformation. These results of the predicted binding geometry are similar to the crystal structure of the Ca^{2+}–clodronate complex. According to previous results, we believe that molecular electrostatic potentials can be safely used to model the calcium binding properties of new candidate compounds in developing new and better bisphosphonate analogs for the treatment of bone diseases, and in understanding the mechanism of action of bisphosphonates. While this level of the theory cannot be expected to yield results of great accuracy, it should be adequate for obtaining qualitative information. It will be very interesting at some future date when computer resources are sufficient to repeat these calculations with larger basis sets and methods which better describe the electronic correlation and especially, to include the solvent molecules in the model systems.

ACKNOWLEDGEMENTS

Financial support for this work from Huhtamäki Oy Leiras, Finland, and support from the Technology Development Centre of Finland (TEKES), is gratefully acknowledged.

REFERENCES

1 Lindroos, J., Thesis for the Degree of Licentiate of Philosophy in Physical Chemistry: The Modeling of Receptor–Ligand Interactions by Quantum Chemical Methods, University of Joensuu, Finland, 1990.
2 Loew, G. and Burt, S. In Hansch, C., Sammes, P.G., Taylor, J.B. and Ramsden, C.A. (Eds.), Comprehensive Medicinal Chemistry, Vol. 4, Quantitative Drug Design, Pergamon Press, Oxford, 1990, p. 116.
3 Goodford, P.J. In Richards, W.G. (Ed.), Computer-Aided Molecular Design, IBC Technical Services Ltd., London, 1989, p. 148.
4 Weinstein, H., Osman, R. and Green, J.P. In Olson, E.C. and Christofferson, R.E. (Eds.), Computer-Assisted Drug Design, ACS Symposium Series 112, American Chemical Society, Washington, D.C., 1979, p. 170.
5 Vinter, J.G., Chem. Br., 21 (1985) 32.
6 Hopfinger, A.J., J. Med. Chem., 24 (1985) 229.
7 Dean, P.M., Molecular Foundations of Drug–Receptor Interaction, Cambridge University Press, Cambridge, 1987, p. 285.
8 Del Re, G., J. Am. Chem. Soc., 80 (1958) 4031.
9 Del Re, G., Pullman, B. and Yonezewa, T., Biochim. Biophys. Acta, 75 (1963) 153.
10 Gasteiger, J. and Marsili, M., Tetrahedron, 36 (1980) 3219.
11 Streitwieser, A. Jr., Molecular Orbital Theory for Organic Chemists, Wiley, New York, 1961.
12 Berthod, H. and Pullman, A., J. Chem. Phys., 62 (1965) 942.
13 Vinter, J.G., Davis, A. and Saunders, M.R., J. Comput.-Aided Mol. Design, 1 (1987) 31.
14 Mulliken, R.S., J. Chem. Phys., 23 (1955) 1833.
15 Dean, P.M., Molecular Foundations of Drug–Receptor Interaction, Cambridge University Press, Cambridge, 1987, p. 76.
16 Clark, T.A., Handbook of Computational Chemistry, Wiley, New York, 1985, p. 241.
17 Fleisch, H. In Handbook of Experimental Pharmacology, Vol. 83, Springer, Berlin/Heidelberg, 1988, p. 441.
18 Jung, A., Bisaz, S., Bartholdi, P. and Fleisch, H., Calcif. Tissue Res., 13 (1973) 27.
19 Francis, M., Russel, R. and Fleisch, H., Science, 165 (1969) 1264.
20 Russel, R., Mühlbauer, R., Bisaz, S., Williams, D. and Fleisch, H., Calcif. Tissue Res., 6 (1970) 183.
21 Gaussian-88 and Gaussian-90, Frisch, M., Head-Gordon, M., Schlegel, H., Rayhavachari, K., Binkley, J., Gonzalez, C., Defrees, D., Fox, D., Whiteside, R., Seeger, R., Melius, C., Baker, J., Martin, R., Kahn, L., Stewart, J., Fluder, E., Topiol, S. and Pople, J., Gaussian Inc., Pittsburgh, PA, U.S.A.
22 Nardelli, M. and Pelizzi, G., Inorg. Chim. Acta, 80 (1983) 259.
23 Dobbs, K.D. and Hehre, W.J., J. Comp. Chem., 7 (1986) 359.
24 SYBYL, versions 5.32 and 5.41, Tripos Associates, Inc., St. Louis, MO, U.S.A.
25 Shiratori, Y. and Nakagawa, S., J. Comp. Chem., 12 (1991) 717.
26 Alexander, R.S., Kanyo, Z.F., Chirlian, L.E. and Christianson, D.W., J. Am. Chem. Soc., 112 (1990) 933.
27 Deerfield, D.W. II, Fox, D.J., Head-Gordon, M., Hiskey, R.G. and Pedersen, L.G., J. Am. Chem. Soc., 113 (1991) 1892.
28 Maynard, A.T., Hiskey, L.G., Pedersen, L.G. and Koehler, K.A., J. Mol. Struct., 124 (1985) 213.
29 Peräkylä, M., Pakkanen, T.A., Björkroth, J.-P. and Pohjala, E., J. Chem. Soc. Perkin Trans 2, in press.